

STUDIES OF CSR AND MICROBUNCHING AT THE JEFFERSON LABORATORY ERLS*

C. Tennant[†], S. Benson, D. Douglas, R. Li

Thomas Jefferson National Accelerator Facility, Newport News, VA 23606, USA

C.-Y. Tsai

SLAC National Accelerator Laboratory, Menlo Park, CA 94025, USA

Abstract

One attractive feature of energy recovery linacs (ERLs) is they are source limited. However as beam brightness increases so too do the effects of coherent synchrotron radiation (CSR) and the microbunching instability. The Low Energy Recirculator Facility at Jefferson Laboratory provides a test bed to characterize aspects of CSR's effect on the beam by measuring the energy extraction via CSR as a function of bunch compression. Data was recorded with acceleration occurring on the rising part of the RF waveform while the full compression point was moved along the backleg of the machine and the response of the beam measured. Acceleration was moved to the falling part of the RF waveform and the experiment repeated. Initial start-to-end simulations using a 1D CSR model show good agreement with measurements. The experiment motivated the design of a modified Continuous Electron Beam Accelerator Facility-style arc with control of CSR and the microbunching gain. Insights gained from that study informed designs for recirculation arcs in an ERL-driven electron cooler for Jefferson Laboratory's Electron Ion Collider. Progress on the design and outstanding challenges of the cooler are discussed.

INTRODUCTION

Coherent synchrotron radiation (CSR) poses a significant challenge for accelerators utilizing high brightness beams. When a bunch travels along a curved orbit, fields radiated from the tail of the bunch can overtake and interact with the head. Rather than the more conventional class of head-tail instabilities where the tail is affected by the actions of the head, CSR is a tail-head instability. The net result is that the tail loses energy while the head gains energy leading to an undesirable redistribution of particles in the bunch. Because the interaction takes place in a region of dispersion, the energy redistribution is correlated with the transverse positions in the bend plane and can lead to projected emittance growth. The following section describes experiments at the Low Energy Recirculator Facility (LERF, formerly the Jefferson Laboratory FEL [1]) to quantify these bulk effects on the bunch distribution. However, in addition to the potential for emittance and energy spread growth, CSR can also drive the microbunching instability. This aspect is

*Authored by Jefferson Science Associates, LLC under U.S. DOE Contract No. DE-AC05-06OR23177, the Office of Naval Research and the High Energy Laser Joint Technology Office. The U.S. Government retains a non-exclusive, paid-up, irrevocable, world-wide license to publish or reproduce this manuscript for U.S. Government purposes.

[†]tennant@jlab.org

addressed later in the context of the Jefferson Laboratory Electron-Ion Collider (JLEIC).

MEASURED EFFECT OF CSR

Studies at the LERF (see Fig. 1) focused on characterizing the impact of CSR with the goal of benchmarking measurements with simulation. The LERF was designed as an energy recovery based linear accelerator used to condition an electron beam for high average power lasing. Electrons are generated in a DC photocathode gun (135 pC), accelerated to 9 MeV and injected into the linac where they are further accelerated up to 130 MeV through three cryomodules. Acceleration nominally occurs 10° ahead of the crest of the RF waveform, to impart a phase-energy correlation across the bunch. The first- and second-order momentum compactions of the first Bates-style recirculation arc are set so that, in conjunction with the downstream chicane, the bunch is rotated upright at the wiggler and phase space curvature is eliminated. Following the wiggler, the longitudinal phase space must be rotated back by 90° to energy compress the beam as it arrives at the dump. The experimental program consisted of characterizing the effects of CSR for two different longitudinal matches: accelerating on the rising (falling) side of RF waveform together with a negative (positive) momentum compaction – from the combined arc and chicane system – for compression.

Accelerating 10° Before Crest

Measurements were made to quantify the effect of parasitic compressions (i.e. when the bunch goes through a full compression) on beam quality through linac-to-wiggler transport. With the nominal energy chirp the beam experiences three such parasitic compressions. Quadrupole scans to measure emittance and Twiss parameters were performed at several locations around the machine and repeated with the linac cross-phased. Cross-phasing refers to switching the accelerating phase of only the middle cryomodule (which has the same gradient as the two outboard cryomodules combined) to the falling side of the RF waveform. Upon exiting the linac the energy chirp is removed and the nearly mono-energetic distribution avoids parasitic compressions. Results of the measurements are summarized in Table 1. The small horizontal emittance growth through the machine for cross-phased measurements is not unexpected, while the effect of parasitic compressions is more dramatic. These measurements together with simulations suggest that while parasitic compressions do not lead to copious CSR-

Content from this work may be used under the terms of the CC BY 3.0 licence (© 2018). Any distribution of this work must maintain attribution to the author(s), title of the work, publisher, and DOI.

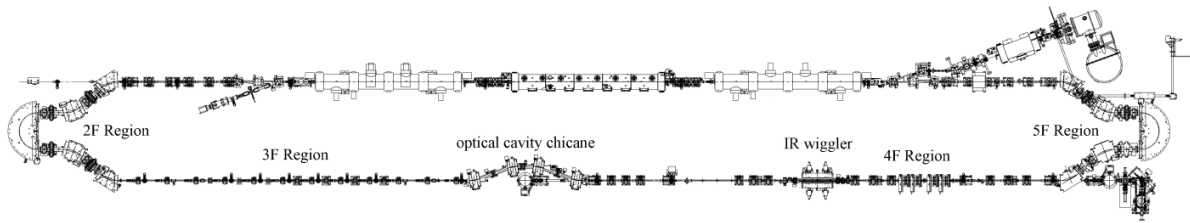


Figure 1: Schematic of the LERF (formerly FEL) without the UV bypass line.

induced energy loss, they do significantly degrade emittance in the bending plane. Simulations using elegant's ultra-relativistic 1D CSR model were unable to generate the observed emittance growth [2]. It is known that the transverse extent of the bunch through the Bates bend violates the so-called "Derbenev criterion" [3] under which the 1D approximation is valid. This, along with the absence of space charge modeling through the arc, may account for the discrepancy.

Table 1: Normalized horizontal emittance and Twiss parameters at various locations in the machine. (0F corresponds to the injector, 2F to the exit of linac, 3F to the exit of first arc and 4F to the exit of the chicane).

| | Cross-Phased | | | Nominal | | |
|----|---------------------------|------------------|------------|---------------------------|------------------|------------|
| | ϵ_x (mm-mrad) | β_x (m) | α_x | ϵ_x (mm-mrad) | β_x (m) | α_x |
| 0F | 15.2 | 11.2 | -0.1 | 15.2 | 11.2 | -0.1 |
| 2F | 17.5 | 11.8 | 6.3 | 17.9 | 12.9 | 6.6 |
| 3F | 20.8 | 3.7 | -1.0 | 30.5 | 3.1 | -0.7 |
| 4F | 21.3 | 11.8 | -5.5 | 41.8 | 16.8 | -8.0 |

Accelerating 10° After Crest

Nominally the R_{56} and T_{566} in the Bates bend are selected (using trim quadrupoles and sextupoles) such that (after traversing a downstream chicane), the bunch is rotated upright at the wiggler. However, it is possible to vary the trim quadrupoles to produce a range of arc linear momentum compactions from -0.5 m to $+1.0$ m. After moving the acceleration to the falling side of the RF waveform, data was recorded of the energy extracted via CSR (measuring BPMs in the dispersive region in the π -bend of the second Bates bend) as function of bunch compression. This is illustrated in Fig. 2. Most energy is extracted when full compression occurs at the optical cavity chicane (left dip) rather than at the end of the arc (right dip). While the R_{56} was varied in the arc, T_{566} was fixed such that the native T_{566} of the chicane corrects the curvature, generating high peak current and exacerbating the effects of CSR [4].

In addition to measuring the CSR-induced energy loss, images from a synchrotron radiation monitor were recorded to capture details of the bunch momentum distribution while the compression state was varied (the synchrotron light monitor is located at a dispersive location where the horizontal beta function is small, effectively mapping the momentum distribution onto the horizontal

axis of the viewer). An animation of the beam response to variable compression is available at [5]. Preliminary start-to-end simulation results show good agreement with measurement, even to the point of replicating observed filamentation on the momentum distribution (see Fig. 3).

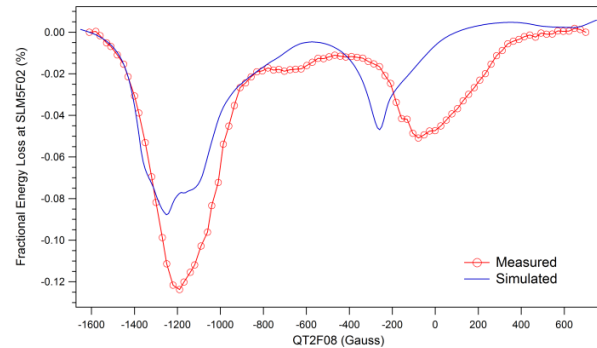


Figure 2: Measured and simulated CSR-induced energy loss as a function of compression state after acceleration on the falling part of the RF waveform.

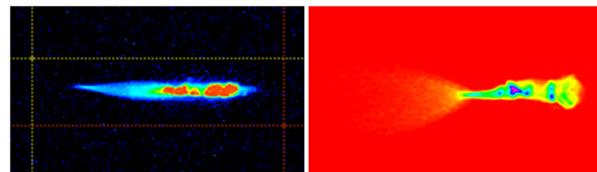


Figure 3: Observed beam momentum distribution modulation (left) compared with simulated results (right).

Figure 4 illustrates changes to the momentum distribution as measured in the second arc (projections plotted along momentum axis) as a function of the compression state (characterized by the strength of one of the quadrupoles varied in the first Bates bend). Two distinct troughs running through the surface plot are clearly discerned. As previously noted, a curved bunch in longitudinal phase space (e.g. when second-order compactions are not properly set) will limit the minimum compressed bunch length and generate one or more localized current spikes. It has been shown that a local concentration of charge can produce stronger CSR wakes than compared to a Gaussian distribution of the same rms length [6]. The strong CSR wake and its effect – namely the redistribution of energy within the distribution – is localized to the region of the current spike which itself moves temporally through the bunch as the compression

state is changed. Note that the regions of depletion correspond to the measured maximum energy loss (compare to Fig. 2).

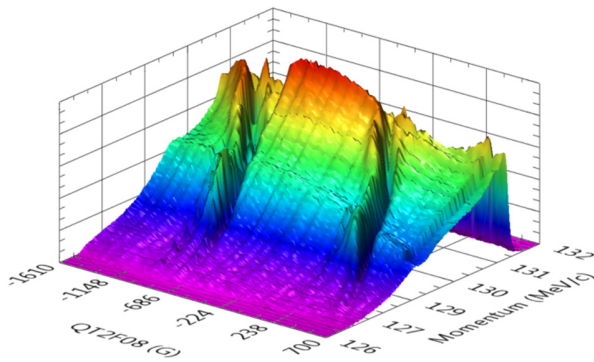


Figure 4: Surface plot illustrating the effects of CSR on the momentum distribution as a function of compression state.

LASING WITH $R_{56} > 0$ COMPRESSION

The FEL itself serves as the best available beam diagnostic. Leveraging the flexibility of the LERF to completely change the longitudinal match, a test was performed of lasing with compression using a positive R_{56} from the linac-to-wiggler transport. Acceleration occurred on the falling side of the RF waveform and signs of the compactions were switched. Lasing was challenged by fact that wiggler gap control firmware was unavailable, keeping the wavelength “stuck” at value for which optical cavity mirrors performed poorly (over 50% losses). Additionally, the “high” reflector had higher transmission than the outcoupler requiring greater than 200% gain just to lase. Despite these issues, the system lased extremely well. After optimization the wavelength was 762 nm with a (10-11) μm detuning curve and a (9.5-10) μs turn-on time – both typical values for the nominally configured system. This proof-of-principle lasing demonstration has important implications for bunch compression, namely:

- 1) Positive compaction is the natural result of bending and is readily achieved in simple beamline configurations (e.g. a FODO arc) supporting simple and effective schemes for aberration compensation, rendering harmonic RF unnecessary.
- 2) Longitudinal space charge (LSC)-induced phase space distortion, on the falling side of the RF waveform, increases the phase-energy correlation on the beam. Thus, LSC enhances the chirp, rather than suppressing it (as occurs on the rising side of the RF waveform), where the suppression can result in a potentially incompressible region of phase space.
- 3) Compressors can be configured – when running with positive compaction – to avoid any spurious over-compression; the final compression occurs in the back end of the final compressor dipole.

The idea of using a compressor arc leads one to contemplate recirculated linac driven light sources. The cost saving benefits of recirculating linacs is well known [7], but concerns about beam degradation, especially due to CSR, through 360° of bending presents a challenge. Progress on an emittance preserving, low microbunching instability (μBI) gain, isochronous arc is discussed below.

EMITTANCE PRESERVING ARC

We apply the compensation analysis of Ref. [8] – as previously used by Borland [9] – to the design of transport systems for use with low emittance beams, and find that appropriately configured second order achromats will suppress transverse emittance growth due to CSR [10]. A second-order achromat composed of superperiods that are individually linearly achromatic and isochronous meet all the requirements for the suppression of CSR effects. In this case, any CSR-induced momentum shift will be paired to a matching shift at a downstream location with the same lattice parameters and the same bunch length. The transverse phase space configuration is “inverted” by the (modulo) half-betatron wavelength phase separation. The impact of the second transverse momentum shift therefore completely cancels (to linear order) that of the first. One such design is for a 1.3 GeV arc based on a modified CEBAF design. Simulation of transport with CSR was performed with elegant. For an initial transverse normalized emittance of 0.25 mm-mrad and assuming an initially upright bunch of length of 3.0 ps and momentum spread 11.7 keV, the emittance is well-preserved over a broad range of bunch charges and initial (rms) bunch lengths. As the beam brightness increases, it is not only the bulk effects of CSR on the bunch, but also the CSR-driven microbunching that must be managed. An unanticipated outcome of the exercise, and of considerable interest, is the additional observation that these beam line designs also manifest little or no evidence of microbunching. In the modified CEBAF arc example, though wake distortion is evident on the longitudinal distributions, there is no visible microbunching until the bunch charge approaches 1.0 nC. Analysis shows micro-bunching gains of less than unity across a range of modulation wavelengths (see Fig. 5) [11].

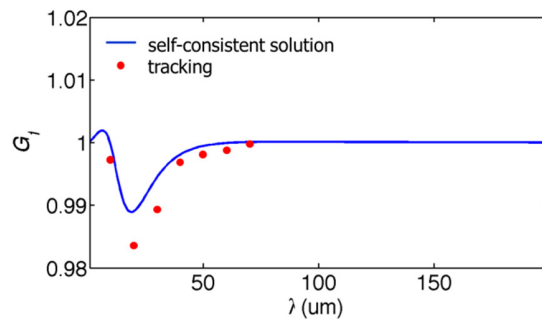


Figure 5: Microbunching gain spectrum as a function of modulation wavelength.

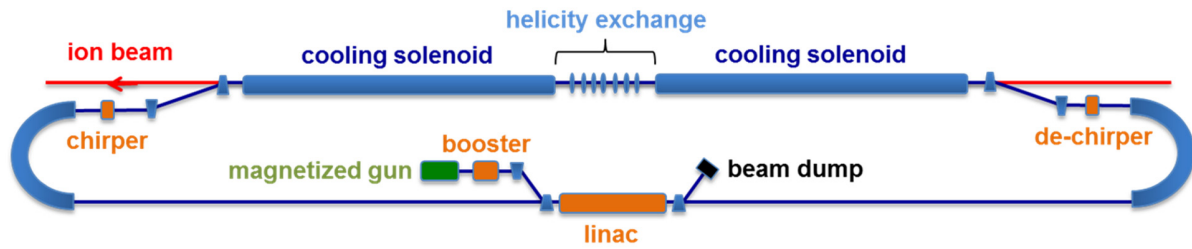


Figure 6: Schematic of the single pass ERL-driven electron cooler for JLEIC.

MICROBUNCHING

The mechanism by which microbunching develops is as follows: an initial density modulation, either from shot noise or from the drive laser, is converted to energy modulations through short-range wakefields such as space charge and CSR. The energy modulations are then transformed back to density modulations through the momentum compaction of the lattice. Danger arises when a positive feedback is formed and the initial modulations are enhanced. This phenomenon has been studied extensively, both theoretically and experimentally, in bunch compressor chicane [12]. Only recently has there been a concerted effort to study the microbunching instability in recirculating arcs [13]. Energy recovery linacs can be particularly susceptible to microbunching. For increased efficiency, ERLs inject beam at low energy and the beam is influenced by space charge forces. Due to the topology required in same-cell energy recovery, ERLs necessarily have substantial bending and are subject to the effects of CSR. And – unlike space charge – the effects of CSR do not diminish at high energy. Because the beam is subject to space charge and/or CSR throughout the machine, density modulations can be converted to energy modulations. And because of the native momentum compaction of the lattice (in arcs, spreaders/recombiners, chicanes, etc.) those energy modulations may be converted back to density modulations. Therefore, for ERLs using high brightness beams, conditions are quite favorable for seeding the microbunching instability.

Studying the microbunching instability in the time-domain (i.e. via particle tracking) presents multiple challenges. The initial density modulation needs to be small enough to remain in the linear regime but large enough to overcome numerical artifacts which requires a large number of particles. Due to the computational burden, it becomes difficult to exercise parametric studies and/or model an entire accelerator complex. On the other hand, a semi-analytical Vlasov solver that works in the frequency-domain and models relevant collective effects such as LSC, CSR and linac geometric effects using analytic impedance expressions has led to insights on lattice constraints for control of the microbunching instability [14]. The development of a fast Vlasov-solver has been an invaluable asset in the design and development of arc lattices.

JLEIC

The U.S. Nuclear Science Advisory Committee has made an electron-ion collider the priority as the next generation of accelerator to serve the nuclear physics community. Jefferson Laboratory's contribution to this effort has been the design of JLEIC, a design over 10 years in the making, which involves colliding polarized electrons (originating from CEBAF) with medium energy ions that would originate in a new ion complex [15]. A ring-ring collider scenario has been chosen as the baseline, with figure-8 shape rings for achieving and preserving the high ion polarization. Calculations indicate that a very high luminosity (over $10^{-34} \text{ cm}^{-2}\text{s}^{-1}$) is possible with the present design concept. However, in order to achieve that ambitious luminosity, several stages of electron beam cooling must be employed. The most challenging is the high energy, bunched beam cooler designed to cool 100 GeV protons. The cooler requires handling a low energy, high power electron beam – which is not unlike a free-electron laser. The primary difference is that an FEL requires a very short (high current) bunch at the interaction region (undulator), whereas the cooler requires a very long, low energy spread bunch at the interaction region (cooling solenoid). Both a strong cooling (baseline) and weak cooling scheme (backup) are being designed. In the following sections, the impact of CSR and microbunching for each are discussed.

Weak Cooling

The weak cooling option is based on an energy recovery linac conditioning a 55 MeV magnetized beam (420 pC/bunch) for a single pass through a long cooling channel (co-propagating with the proton beam) before the beam energy is recovered. A schematic of the machine is shown in Fig. 6. Effective cooling requires preserving the transverse emittance and meeting the energy spread specification of 3×10^{-4} (rms). The recirculation arcs are comprised of index- $\frac{1}{2}$ dipoles to maintain axial symmetry and preserve the magnetization. The arc is tuned to have a R_{56} of +0.55 m so as to debunch the beam and lengthen it from 20 ps (full) to 67 ps (full). The computer code TStep was used to model space charge and CSR in the arc and its effect on the beam. Results show a 2% growth in the transverse emittance. The wake-induced distortions along the bunch are modest and should present no challenges in achieving the required energy spread at the cooling

channel. Recent efforts have studied the effect of transporting a magnetized beam on the microbunching gain [16]. It turns out that the relatively large transverse size (on the order of millimeters) produces a smearing effect, analogous to Landau damping when the energy spread is large, which effectively damps the instability. Using the fast Vlasov-solver we can quickly estimate the microbunching gain curve. We note that the Vlasov solver has been extensively benchmarked with the more computationally intensive and tedious particle tracking in elegant. The result shows that the microbunching instability is well controlled over a large range of incoming intrinsic energy spreads; it is damped by the arc (gain < 1) when $\delta p/p = 2.4 \times 10^{-3}$ and is near unity for $\delta p/p = 8 \times 10^{-5}$.

Strong Cooling

Rather than the single pass ERL, the new baseline is a circulator cooling ring (CCR) driven by an ERL. The idea is that an ERL, conceptually similar to the one designed for weak cooling, accelerates 2 to 3.2 nC bunches to 55 MeV/c. After the first arc, the cooling channel is replaced by a beam exchanger where the bunch is kicked upward into a CCR. The bunch will make 10 to 20 turns in the CCR wherein it will pass through a cooling channel on every revolution. A kicker [17] then directs the beam back down to the ERL where the bunch is energy recovered. As in the weak cooling design, the bunch delivered to the cooling channel must be long (with a flattop distribution of full length 2 cm) and of small relative momentum spread (3×10^{-4} rms). In addition to preserving the beam quality through the first arc of the ERL and the beam exchange region, one of the biggest challenges is maintaining a sufficiently small energy spread while the bunch is subjected to the CSR wake over the course of 20 turns in the CCR. While methods to mitigate the transverse emittance growth have already been explored, the energy loss and gross distortion along the bunch from the CSR wake are not easily reversed. The CSR wake is proportional to the bunch distribution. For a flattop the effect of the wake is impart a fairly linear slope across the bunch. Simulations using an RF cavity run near zero-crossing to both remove the slope and restore the energy loss from CSR have been moderately successful (see Fig. 7). Estimates suggest that CSR shielding can be effective and will be explored as arc designs mature.

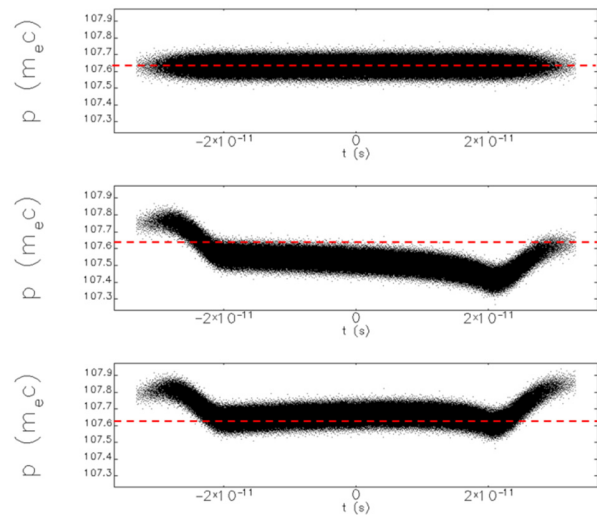


Figure 7: Initial longitudinal phase space (top) and after one turn in the CCR with CSR without correction (middle) and with correction via an RF cavity (bottom).

SUMMARY

In Jefferson Laboratory's three ERL-driven FELs (IR Demo, IR Upgrade, UV) CSR has been present though has never as an operational impediment. As we look toward the future and consider an ERL-driven cooler with higher bunch charges, CSR as well as the microbunching instability become challenges to be addressed in the design of arcs. This leads to an important point, namely that we are approaching the limits of what currently available simulation codes can handle. We are entering a low energy, high charge region of parameter space where both space charge and CSR are important. Furthermore, initial studies have shown that the ability to simulate the effect of CSR shielding is going to be a high priority.

REFERENCES

- [1] C. Tennant, Proc. PAC'09, pp. 3125-3129 (2009).
- [2] M. Borland, Advanced Photon Source LS-287 (2000).
- [3] Y.S. Derbenev et al., TESLA FEL Report 1995-05 (1995).
- [4] C. Hall et al., Phys. Rev. ST Accel. Beams **18**, 030706 (2015).
- [5] <https://goo.gl/KoIcpu>
- [6] R. Li, NIM-A, **475** 498-503 (2001).
- [7] R. York, PRST-AB **17**, 010705 (2014).
- [8] S. DiMitri et al., Phys. Rev. Lett. **110**, 014801 (2013).
- [9] M. Borland et al., Proc. AccApp'07, pp. 196-203 (2007).
- [10] D. Douglas et al., arXiv:1403.2318 (2014).
- [11] C.-Y. Tsai et al., Proc. 36th FEL Conference, pp. 730-734 (2014).
- [12] S. Heifets et al., Phys. Rev. ST Accel. Beams **5**, 064401 (2002).
 Z. Huang and K.-J. Kim, Phys. Rev. ST Accel. Beams **5**, 074401 (2002).

- [13] S. DiMitri and M. Cornacchia, EPL, **109** 62002 (2015).
C.-Y. Tsai et al., Phys. Rev. Accel. Beams **19**, 114401 (2016).
C.-Y. Tsai et al., Phys. Rev. Accel. Beams **20**, 024401 (2017).
- [14] C.-Y. Tsai et al., Phys. Rev. Accel. Beams **20**, 024401 (2017).
- [15] S. Abeyratne et al., arXiv:1504.07961 (2015).
- [16] C.-Y. Tsai et al., Phys. Rev. Accel. Beams **20**, 054401 (2017).
- [17] Y. Huang et al., Phys. Rev. Accel. Beams **19**, 122001 (2016).